International Journal of Mathematical Archive-3(5), 2012, 1967-1977
Available online through www.ijma.info ISSN 2229 – 5046

FINITE ELEMENT ANALYSIS OF MIXED CONVECTIVE HEAT AND MASS TRANSFER FLOW IN A CONCENTRIC CYLINDRICAL ANNULUS

Dr. Y. Madhusudhana Reddy[1*], Prof. D.R.V. Prasada Rao[2] and P. Sreenivasa Rao[3]

[1]Associative Professor, Dept. of Mathematics, Sri venkateswara Institute of Technology, Anantapur, Andhrapradesh, India

[2]Professor, Dept of Mathematics, S. K. University, Anantapur, Andhrapradesh, India

[3]Dept of Physics, Jyothirmai Engineering College, Karimnagar. Andhrapradesh, India

(Received on: 11-05-12; Accepted on: 31-05-12)

ABSTRACT

The mixed convective heat and mass transfer flow of a viscous fluid through a porous medium in cylindrical annulus is considered. The non coupled equations governing the heat and mass transfer are solved by employing a finite element analysis. The effect of various fluid forces on the velocity, temperature, concentration is analyzed. The rate of heat and mass transfer on the inner and outer cylinders are evaluated numerically for different parametric values.

Key words*: Mixed convective heat and mass transfer flow, porous medium, Galarkin finite element analysis.*

1. INTRODUCTION

Free convection in a vertical porous annulus has been extensively studied by Prasad [7] both theoretically and experimentally. Convection through annulus region under steady state conditions has also been discussed with two cylindrical surface kept at different temperatures [8]. This work has been extended in temperature dependent convection flow as well as convection flows through horizontal porous channel whose inner surface is maintained at constant temperature while the other surface is maintained at circumferentially varying sinusoidal temperature[9]. Free convection flow and heat transfer in hydromagnetic case is important in nuclear and space technology.

Chen and Yuh [3] have investigated the heat and mass transfer characteristics of natural convection flow along a vertical cylinder under the combined buoyancy effects of thermal and species diffusion. Sivanjaneya Prasad [11] has investigated the free convection flow of an incompressible, viscous fluid through a porous medium in the annulus between the porous concentric cylinders under the influence of a radial magnetic field. Antonio[2] has investigated the laminar flow, heat transfer in a vertical cylindrical duct by taking into account both viscous dissipation and the effect of buoyancy, The limiting case of fully developed natural convection in porous annuli is solved analytically for steady and transient cases by E. Sharawi and Al-Nimir[10] and Al-Nimir [1]. Philip [6] has obtained solutions for the annular porous media valid for low modified Reynolds number. Ravi [8] has analysed the unsteady convective heat and mass transfer through a cylindrical annulus with constant heat sources. Sreevani [13] has studied the convective heat and mass transfer through a porous medium in a cylindrical annulus under radial magnetic field with Soret effect. Prasad [7] has analysed the convective heat and mass transfer in an annulus in the presence of heat generating source under radial magnetic field. Reddy [12] has discussed the Soret effect on mixed convective heat and mass transfer through a porous cylindrical annulus. For natural convection, the existence of large temperature differences between the surfaces is important. Keeping the applications in view, Sudheer Kumar et al [15] have studied the effect of radiation on natural convection over a vertical cylinder in a porous media. Padmavathi [5] has analyzed the convective heat transfer in a cylindrical annulus by using finite element method.

In this paper we discuss the free and forced convection flow through a porous medium in a co-axial cylindrical duct where the boundaries are maintained at constant temperature and concentration. The Brinkman Forchhimer extended Darcy equations which takes into account the boundary and inertia effects are used in the governing linear momentum equations. The effect of density variation is confined to the buoyancy term under Boussinesq approximation. The momentum, energy and diffusion equations are coupled equations. In order to obtain a better insight into this complex problem, we make use of Galerkin finite element analysis with quadratic polynomial approximations. The Galerkin finite element analysis has two important features. The first is that the approximation solution is written directly as a

Corresponding author: *Dr. Y. Madhusudhana Reddy[1*]*
[1]Associative Professor, Dept. of Mathematics, Sri venkateswara Institute of Technology, Anantapur,(A.P.), India

linear combination of approximation functions with unknown nodal values as coefficients. Secondly, the approximation polynomials are chosen exclusively from the lower order piecewise polynomials restricted to contiguous elements. The behaviour of velocity, temperature and concentration is analysed at different axial positions. The shear stress and the rate of heat and mass transfer have also been obtained for variations in the governing parameters.

2. FORMULATION OF THE PROBLEM

We consider the free and forced convection flow in a vertical circular annulus through a porous medium whose walls are maintained at a constant temperature and concentration. The flow, temperature and concentration in the fluid are assumed to be fully developed. Both the fluid and porous region have constant physical properties and the flow is a mixed convection flow taking place under thermal and molecular buoyancies and uniform axial pressure gradient. The Boussenissq approximation is invoked so that the density variation is confined to the thermal and molecular buoyancy forces. The Brinkman-Forchhimer-Extended Darcy model which accounts for the inertia and boundary effects has been used for the momentum equation in the porous region. The momentum, energy and diffusion equations are coupled and non-linear. Also the flow is unidirectional along the axial direction of the cylindrical annulus. Making use of the above assumptions the governing equations are

$$-\frac{\partial p}{\partial z}+\frac{\mu}{\delta}\left(\frac{\partial^2 u}{\partial r^2}+\frac{1}{r}\frac{\partial u}{\partial r}\right)-\frac{\mu}{k}u-\frac{\rho\delta F}{\sqrt{k}}u^2+\rho g\beta(T-T_0)+\rho g\beta^{\bullet}(C-C_0)=0 \tag{1}$$

$$\rho c_p u\frac{\partial T}{\partial z}=\lambda\left(\frac{\partial^2 T}{\partial r^2}+\frac{1}{r}\frac{\partial T}{\partial r}\right)+Q \tag{2}$$

$$u\frac{\partial C}{\partial z}=D_1\left(\frac{\partial^2 C}{\partial r^2}+\frac{1}{r}\frac{\partial C}{\partial r}\right) \tag{3}$$

where u is the axial velocity in the porous region, T , C are the temperature and concentration of the fluid, k is the permeability of porous medium, F is a function that depends on Reynolds number, the microstructure of the porous medium and D_1 is the molecular diffusivity, β is the coefficient of the thermal expansion, β* is the coefficient of volume expansion, Cp is the specific heat, ρ is density and g is gravity.

The relevant boundary conditions are

$u=0$, $T=T_i$, $C=Ci$ at r = a
$u=0$, $T=T_0$, $C=Co$ at r = a+s (4)

We now define the following non-dimensional variables

$$z^*=\frac{z}{a},\quad r^*=\frac{r}{a},\quad u^*=\frac{a}{\gamma}u$$
$$p^*=\frac{pa\delta}{\rho\gamma^2},\quad \theta^*=\frac{T-T_0}{T_i-T_0},\quad s^*=\frac{s}{a}$$
$$C^*=\frac{C-C_0}{C_i-C_0}$$

Introducing these non-dimensional variables, the governing equations in the non-dimensional form are (on removing the stars)

$$\frac{\partial^2 u}{\partial r^2}+\frac{1}{r}\frac{\partial u}{\partial r}=\pi+\delta(D^{-1})u+\delta^2\Lambda u^2-\delta G(\theta+N\,C) \tag{5}$$

$$\frac{\partial^2\theta}{\partial r^2}+\frac{1}{r}\frac{\partial\theta}{\partial r}=P_r N_1 u \tag{6}$$

$$\frac{\partial^2 C}{\partial r^2}+\frac{1}{r}\frac{\partial C}{\partial r}=Sc\,N_2 u \tag{7}$$

where

$\Lambda = FD^{-1}$ (Inertia parameter), $G=\dfrac{g\beta(T_1-T_0)a^3}{\gamma^2}$ (Grashoff number)

$D^{-1}=\dfrac{a^2}{k}$ (Inverse Darcy parameter), $N_1=\dfrac{Aa}{T_1-T_0}$ (Non-dimensionaltemperature gradient)

$N_2=\dfrac{Ba}{C_1-C_0}$ (Non-dimensional concentration gradient), $P_r=\dfrac{\rho c_p \gamma}{\lambda}$ (Prandtl number)

$Sc=\dfrac{\nu}{D_1}$ (Schmidt number)

The corresponding non-dimensional conditions are

$u=0,\theta=1$, C=1 at r=1 (8)

$u=0,\theta=0$, C=0 at r=1+s (9)

For N=0 the equations (5) – (8) reduce to that of padmavathi [5].

3. FINITE ELEMENT ANALYSIS

The finite element analysis with quadratic polynomial approximation functions is carried out along the radial distance across the circular duct. The behavior of the velocity, temperature and concentration profiles has been discussed computationally for different variations in governing parameters. The Gelarkin method has been adopted in the variational formulation in each element to obtain the global coupled matrices for the velocity, temperature and concentration in course of the finite element analysis. Choose an arbitrary element e_k and let u^k, θ^k and C^kbe the values of u, θ and C in the element e_k We define the error residuals as

$$E_p^k=\frac{d}{dr}\left(r\frac{du^k}{dr}\right)+\delta G(\theta^k+NC^k)-\delta(D^{-1})ru^k-\delta^2\Lambda r(u^k)^2 \tag{10}$$

$$E^k{}_\theta=\frac{d}{dr}\left(r\frac{d\theta^k}{dr}\right)-rP_rN_1u^k \tag{11}$$

$$E^k{}_c=\frac{d}{dr}\left(r\frac{dC^k}{dr}\right)-rScN_2u^k \tag{12}$$

where u^k, θ^k & C^k are values of u, θ& C in the arbitrary element e_k. These are expressed as linear combinations in terms of respective local nodal values.

$$u^k=u_1^k\psi_1^k+u_3^k\psi_1^k+u_3^k\psi_3^k$$
$$\theta^k=\theta_1^k\psi_1^k+\theta_2^k\psi_2^k+\theta_3^k\psi_3^k$$
$$C^k=C_1^k\psi_1^k+C_2^k\psi_2^k+C_3^k\psi_3^k$$

where ψ_1^k, ψ_2^k --------- etc are Lagrange's quadratic polynomials.

Following the Gelarkin weighted residual method and integrating by parts equations (10) - (12) we obtain

$$\int_{rA_1}^{rB_1} r\frac{du^k}{dr}\frac{d\psi_j^k}{dr}dr-\delta G\int_{rA_1}^{rB_1} r(\theta^k+NC^k)\psi_j^k dr+\delta(M_1{}^2)\int_{rA_1}^{rB_1} ru^k\psi_j^k dr+\delta^2\Lambda\int_{rA_1}^{rB_1} r(u^k)^2\psi_j^k dr=Q_{2\,j}^k+Q_{1\,j}^k-P\int_{rA_1}^{rB_1} r\psi_j^k dr \tag{13}$$

$$-Q_{1\,j}^{k}=\left[\left(\frac{du^{k}}{dr}\right)(r\psi_{j}^{k})\right]r_{A_1},\quad -Q_{2\,j}^{k}=\left[\left(\frac{du^{k}}{dr}\right)(r\psi_{j}^{k})\right]r_{B_1}$$

$$\int_{rA_1}^{rB_1} r\frac{du^{k}}{dr}\frac{d\psi_{j}^{k}}{dr}dr=N_1P_r\int_{rA_1}^{rB_1} ru^{k}\psi_{j}^{k}dr+R_{2\,j}^{k}+R_{1\,j}^{k}-R_{1\,j}^{k}=\left[\left(\frac{d\theta^{k}}{dr}\right)(r\psi_{j}^{k})\right]r_{A_1}.R_{2\,j}^{k}=\left[\left(\frac{d\theta^{k}}{dr}\right)(r\psi_{j}^{k})\right]r_{B_1} \quad (14)$$

$$\int_{rA_1}^{rB_1} r\frac{du^{k}}{dr}\frac{d\psi_{j}^{k}}{dr}dr=N_2Sc\int_{rA_1}^{rB_1} ru^{k}\psi_{j}^{k}dr+S_{2\,j}^{k}+S_{1\,j}^{k}-S_{1\,j}^{k}=\left[\left(\frac{dC^{k}}{dr}\right)(r\psi_{j}^{k})\right]r_{A_1}S_{2\,j}^{k}=\left[\left(\frac{dC^{k}}{dr}\right)(r\psi_{j}^{k})\right]r_{B_1} \quad (15)$$

Expressing uk, θ^k, C^k in terms of local nodal values in (13) - (15) we obtain

$$\sum_{i=1}^{3}u^{k}\int_{rA_1}^{rB_1} r\frac{d\psi_{i}^{k}}{dr}\frac{d\psi_{j}^{k}}{dr}dr-\delta G\sum_{i=1}^{3}(\theta_{i}^{k}+NC_{i}^{k})\int_{rA_1}^{rB_1} r\psi_{i}^{k}\psi_{j}^{k}dr+\delta D^{-1}\sum_{i=1}^{3}\int_{rA_1}^{rB_1} r\psi_{i}^{k}\psi_{j}^{k}dr$$
$$+\delta^{2}\Lambda\sum_{i=1}^{3}u_{i}^{k}\int_{rA_1}^{rB_1} rU_{i}^{k}\psi_{i}^{k}\psi_{j}^{k}dr=Q_{2\,j}^{j}+Q_{1\,j}^{k}-P\int_{rA_1}^{rB_1} r\psi_{i}^{k}\psi_{j}^{k}dr \quad (16)$$

$$\sum_{i=1}^{3}\theta_{i}^{k}\int_{rA_1}^{rB_1} r\frac{d\psi_{i}^{k}}{dr}\frac{d\psi_{j}^{k}}{dr}dr-N_1P_r\sum_{i=1}^{3}u_{i}^{k}\int_{rA_1}^{rB_1} r\psi_{i}^{k}\psi_{j}^{k}dr=R_{2\,j}^{k}+R_{1\,j}^{k} \quad (17)$$

$$\sum_{i=1}^{3}C_{i}^{k}\int_{rA_1}^{rB_1} r\frac{d\psi_{i}^{k}}{dr}\frac{d\psi_{j}^{k}}{dr}dr-N_2Sc\sum_{i=1}^{3}u_{i}^{k}\int_{rA_1}^{rB_1} r\psi_{i}^{k}\psi_{j}^{k}dr=S_{2\,j}^{k}+S_{1\,j}^{k} \quad (18)$$

$$M_1^2=\mathrm{D}^{-1} \quad (19)$$

Choosing different ψ_j^k's corresponding to each element e_k in the equation (16) yields a local stiffness matrix of order 3×3 in the form

$$(f_{i\,j}^{k})(u_{i}^{k})-\delta G(g_{i\,j}^{k})(\theta_{i}^{k}+NC_{i}^{k})+\delta D^{-1}(m_{i\,j}^{k})(u_{i}^{k})+\delta^{2}\Lambda(n_{i\,j}^{k})(u_{i}^{k})=(Q_{2\,j}^{k})+(Q_{1\,j}^{k})+(v_{j}^{k}) \quad (20)$$

Likewise the equation (3. 8) & (3. 9) give rise to stiffness matrices

$$(e_{i\,j}^{k})(\theta_{i}^{k})-N_1P_r(t_{i\,j}^{k})(u_{i}^{k})=R_{2\,j}^{k}+R_{1\,j}^{k} \quad (21)$$

$$(l_{i\,j}^{k})(C_{i}^{k})-N_2c(t_{i\,j}^{k})(u_{i}^{k})=S_{2\,j}^{k}+S_{1\,j}^{k} \quad (22)$$

where

$(f_{i\,j}^{k})$, $(g_{i\,j}^{k})$, $(m_{i\,j}^{k})$, $(n_{i\,j}^{k})$, $(e_{i\,j}^{k})$, $(l_{i\,j}^{k})$ and $(t_{i\,j}^{k})$ are 3×3 matrices and $v_{j}^{k}=-P_1\int_{rA_1}^{rB_1} r\psi_{i}^{k}\psi_{j}^{k}dr$

and $(Q_{2\,j}^{k})$, $(Q_{1\,j}^{k})$, $(R_{2\,j}^{k})$ & $(R_{1\,j}^{k})$, $(S_{2\,j}^{k})$ & $(S_{1\,j}^{k})$ are 3×1 column matrices. Such stiffness matrices (20) - (22) in terms of local nodes in each element are assembled using interelement continuity and equilibrium conditions to obtain the coupled global matrices in terms of the global nodal values of u , θ & C in the region.

In case we choose n quadratic elements, then the global matrices are of order 2n+1. The ultimate coupled global matrices are solved to determine the unknown global nodal values of the velocity, temperature and concentration in

fluid region. In solving these global matrices an iteration procedure has been adopted to include the boundary and effects in the porous medium.

In fact, the non-linear term arises in the modified Brinkman linear momentum equation (13) of the porous medium. The iteration procedure in taking the global matrices is as follows. We split the square term into a product term and keeping one of them say U_i's under integration, the other is expanded in terms of local nodal values as in (16), resulting in the corresponding coefficient matrix $(n^k_{i\ j}'s)$ in (20), whose coefficients involve the unknown U_i's . To evaluate (20), to begin with, choose the initial global nodal values of U_i's as zeros in the zeroth approximation. We evaluate u_i's , θ_i's and C_i's in the usual procedure mentioned earlier. Later choosing these values of u_i's as first order approximation calculate θ_i's, C_i's. In the second iteration, we substitute for U_i's the first order approximation of and u_i's and the first approximation of θ_i's and C_i's and obtain second order approximation. This procedure is repeated till the consecutive values of u_i's , θ_i's and C_i's differ by a preassigned percentage.

The equilibrium conditions are

$$\begin{aligned}
&R_3^1 + R_1^2 = 0, && R_3^2 + R_1^3 = 0,\ R_3^3 + R_1^4 = 0, && R_3^4 + R_1^5 = 0,\\
&Q_3^1 + Q_1^2 = 0, && Q_3^2 + Q_1^3 = 0,\ Q_3^3 + Q_1^4 = 0, && Q_3^4 + Q_1^5 = 0,\\
&S_3^1 + S_1^2 = 0, && S_3^2 + S_1^3 = 0,\ S_3^3 + S_1^4 = 0, && S_3^4 + S_1^5 = 0
\end{aligned} \qquad (23)$$

4. SOLUTION OF THE PROBLEM

Solving these coupled global matrices for temperature, concentration and velocity respectively and using the iteration procedure we determine the unknown global nodes through which the temperature, concentration and velocity at different radial intervals at any arbitrary axial cross sections are obtained. The respective expressions are given by

$$\begin{aligned}
\theta(r) &= \psi_1^1\,\theta_{11} + \psi_{21}^1\,\theta_{12} + \psi_3^1\,\theta_{13} && 1 \le r \le 1 + S*0.2\\
&= \psi_1^2\,\theta_{13} + \psi_2^2\,\theta_{14} + \psi_3^2\,\theta_{15} && 1 + S*0.2 \le r \le 1 + S*0.4\\
&= \psi_1^3\,\theta_{15} + \psi_2^3\,\theta_{16} + \psi_3^3\,\theta_{17} && 1 + S*0.4 \le r \le 1 + S*0.6\\
&= \psi_1^4\,\theta_{17} + \psi_2^4\,\theta_{18} + \psi_3^4\,\theta_{19} && 1 + S*0.6 \le r \le 1 + S*0.8\\
&= \psi_1^{15}\,\theta_{19} + \psi_2^5\,\theta_{20} + \psi_3^5\,\theta_{21} && 1 + S*0.8 \le r \le 1 + S
\end{aligned}$$

$$\begin{aligned}
C(r) &= \psi_1^1\,C_{11} + \psi_{21}^1\,C_{12} + \psi_3^1\,C_{13} && 1 \le r \le 1 + S*0.2\\
&= \psi_1^2\,C_{13} + \psi_2^2\,C_{14} + \psi_3^2\,C_{15} && 1 + S*0.2 \le r \le 1 + S*0.4\\
&= \psi_1^3\,C_{15} + \psi_2^3\,C_{16} + \psi_3^3\,C_{17} && 1 + S*0.4 \le r \le 1 + S*0.6\\
&= \psi_1^4\,C_{17} + \psi_2^4\,C_{18} + \psi_3^4\,C_{19} && 1 + S*0.6 \le r \le 1 + S*0.8\\
&= \psi_1^{15}\,C_{19} + \psi_2^5\,C_{20} + \psi_3^5\,C_{21} && 1 + S*0.8 \le r \le 1 + S
\end{aligned}$$

$$\begin{aligned}
u(r) &= \psi_1^1\,u_{11} + \psi_{21}^1\,u_{12} + \psi_3^1\,u_{13} && 1 \le r \le 1 + S*0.2\\
&= \psi_1^2\,u_{13} + \psi_2^2\,u_{14} + \psi_3^2\,u_{15} && 1 + S*0.2 \le r \le 1 + S*0.4\\
&= \psi_1^3\,c_{15} + \psi_2^3\,c_{16} + \psi_3^3\,c_{17} && 1 + S*0.4 \le r \le 1 + S*0.6\\
&= \psi_1^4\,u_{17} + \psi_2^4\,u_{18} + \psi_3^4\,u_{19} && 1 + S*0.6 \le r \le 1 + S*0.8\\
&= \psi_1^{15}\,u_{19} + \psi_2^5\,u_{20} + \psi_3^5\,u_{21} && 1 + S*0.8 \le r \le 1 + S
\end{aligned}$$

5. NUSSELT NUMBER AND SHERWOOD NUMBER

The rate of heat transfer (Nusselt number) is evaluated using the formula

$$Nu = -\left(\frac{d\theta}{dr}\right)_{r=1,1+s}$$

The rate of mass transfer (Sherwood number) is evaluated using the formula

$$Sh = -(\frac{dC}{dr})_{r=1,1+s}$$

6. DISCUSSION OF THE NUMERICAL RESULTS

In this analysis we investigate the non-darcy convective heat and mass transfer flow of a viscous fluid in the annular region within the two concentric cylinders which are maintained at constant temperature and concentrations. By using Galerkin finite element analysis with quadratic polynomials, the velocity, temperature and concentration have been analyzed for different values of the governing parameter D^{-1} (Darcy Parameter, N(buoyancy ratio), S_c(Schmidt Number.) N_1&N_2(temperature and concentration gradient) respectively. From fig-1 we notice that the variation of u is remarkably appreciable for higher values of D^{-1}. Lesser the permeability of the porous medium larger |u| and for further lowering of the permeability higher u in the region $1.1 \geq r \leq 1.4$ and smaller u in the region 1.5 to 1.9. The variation of u with buoyancy ratio N reveals that u exhibits a reversal flow in the entire region for N= -0.5 and no such flow exists anywhere in the region for any value of |N|. Also when the molecular buoyancy force dominates over the thermal buoyancy force, the axial velocity experiences depreciation in flow field irrespective of the directions of the buoyancy forces (fig-2). Fig-3 represents the variation of u with Sc fixing the other parameters. It is found that lesser the molecular diffusivity smaller the axial velocity in the entire flow field. The variation of u with temperature gradient N_1 and concentration gradient N_2 shows that an increase in temperature gradient N_1/concentration gradient N_2 results is an enhancement in u everywhere in the region (fig4).

Figures 5-8 represent the variation of θ with D^{-1}, Sc, So, N1 & N_2. From fig 5 we notice that lesser the permeability of the porous medium smaller the actual temperature in the region (1.1- 1.4) and larger the actual concentration in the region (1.5 - 1.9) and for further lowering of the permeability larger the actual temperature in the flow field except in the region (1.5 - 1.7) where it experience a depreciation. When the molecular buoyancy force dominates over the thermal buoyancy force the actual temperature experiences an enhancement with buoyancy forces in the same directions while for the forces in the opposite directions it experiences depreciation in the flow region (fig-6). From fig-7 we notice that lesser the molecular diffusivity larger the actual temperature in the flow phenomena. With reference to variation of θ with N_1 & N_2 we notice that there is appreciable change in the actual temperature with concentration gradient N_2. An increase $N_1 \leq 0.5$ results in an enhancements in actual temperature and for higher $N_1 \geq 0.75$ we notice depreciation in actual temperature. An increase in N_2 leads to a reduction in the actual temperature everywhere in the flow region (fig-8).

The Non-dimensional concentration distribution (C) is exhibited in figs 9-12 for different parameters D^{-1}, S_c, N, N_1 & N_2. Lesser the permeability of the porous medium lesser the actual concentration in the left half and larger it in the right half and for still lowering of the permeability larger the concentration everywhere in the region.(fig-9). When the molecular buoyancy force dominates over the thermal buoyancy force the actual concentration enhances when the buoyancy forces acting in the same direction while for the forces acting in opposite directions it reduces everywhere in the region (fig-10). The variation of θ with S_c indicates that C is negative for smaller and higher values of S_c and is positive for intermediate values. It is found that the actual concentration enhances in the region (1.1-1.4) and depreciates in (1.5-1.9). We notice a remarkable depreciation in actual concentration for smaller values of Sc (fig-11). Fig-12 represents the variation of C with N_1 & N_2. It is found that θ is negative for all N_1 & N_2 except for N_1=0.75. The actual concentration enhances with $N_1 \leq 0.5$ and depreciates with higher $N_1 > 0.75$. An increase in $N_2 \geq 0.5$ leads to a depreciation in the actual concentration with N_2=0.5 and for higher $N_2 \geq 0.75$ we notice an enhancement in the actual concentration.

The Nusselt Number (Nu) which measures the rate of heat transfer at the inner and outer cylinder is shown in table 1-4. It is found that the rate of heat transfer depreciates in magnitude with increase in |G| at both the boundaries. Lesser the permeability of the porous medium smaller |Nu| at r=1and 2. Also lesser the molecular diffusivity larger the rate of heat transfer at both the cylinders. When the molecular buoyancy force dominates over the thermal buoyancy force |Nu| enhances when the buoyancy forces act in the same direction, while for the forces acting in opposite direction its depreciate at both the boundaries(tables 1 &3). From tables 2 & 4, An increase in N_1 enhances |Nu| at r=1 and reduces it at r=2, while it enhances at both the boundaries with increase in N_2.

The Sherwood Number (Sh) which measure the rate of mass transfer at r=1and2 is shown in tables 5-8 for different values of the parameters. It is noticed that the rate of mass transfer is positive for all variations. The rate of mass transfer enhances at r=1 and reduces at r=2 with increase in G>0 while an increase in G<0 reduces it r=1 and enhances it at r=2. The variation of Sh with D^{-1} shows that lesser the permeability of the porous medium larger Sh at r=1 and smaller Sh at r=2. Also lesser the molecular diffusivity larger Sh at r=1 and smaller Sh at r=2. The variation of Sh with buoyancy ratio N shows that when the molecular buoyancy force dominate over the thermal buoyancy force, the rate of mass transfer reduces at r=1 and enhances at r=2 when the buoyancy forces act in the same direction while for the

forces acting in opposite directions it enhances at r=1 and depreciates at r=2(tables 5 & 11). The rate of mass transfer at inner cylinder r=1 depreciate with N_1 and enhances with N_2 while at outer cylinder r=2 it enhances with N_2 and increase with N_2(table 6&8) In general, we find that the rate of mass transfer at inner cylinder r=1 is greater that that r=2.

7. REFERENCES

[1] Al. Nimr, M. A: Analytical solutions for transient laminar fully developed free convection in vertical annuli. Int. J. Heat and Mass Transfer (1993), V. 36, pp. 2388-2395.

[2] Antonio Barletle,: Combined forced and free convection with viscous dissipation in a vertical duct., Int. J. Heat and Mass Transfer, (1999), V. 42, pp.2243-2253.

[3] Chen, T. S and Yuh, C. F,: Combined heat and mass transfer in natural convection on inclined surface., J. Heat Transfer,(1979), V. 2, pp. 233-250.

[4] K.Bharathi, Convective heat and mass transfer through a porous medium in channels/pipes with radiation and Soret effect, (2007)., Ph. D thesis, S.K University, Anantapur ,

[5] Padmavathi, A: "Finite element analysis of non – darcian convective heat transfer through a porousmedium in cylindrical& rectangular ducts with heat generating sources and radiation" (2009) Ph. D thesis, S. K. University, Anantapur, India,

[6] Philip, J. R: Axisymmetric free convection at small Rayleigh numbers in porous cavities. Int. J. Heat and Mass Transfer,(1982), V. 25, pp. 1689-1699.

[7] Prasad, V: Natural convection in porous media,(1983) , Ph. D thesis , S. K. University, Anantapur, India.

[8] Ravi, A: Unsteady convection heat and mass transfer flow through a porous medium in wavy channels (2003), Ph. D thesis, S. K. University, Anantapur, India.

[9] Robillard, L Ngugen, T, H, Sathish, M. G ans Vasseur, P:Heat transfer in porous media and particulate flows, HTD-V, (1985) 46, p. 41. ASME,

[10] Shaarawi, El. M. A. I and Al-Nimir, M.:Fully developed laminar natural convection in open ended vertical concentric annuli. , Int. J. Heat and Mass Transfer , (1999),pp. 1873- 1884.

[11] Sivanjaneya Prasad , P:Effects of convection heat and mass transfer in unsteady hydromagnetic channels flow, (2001), Ph. D thesis, S. K. University, Anantapur, India,

[12] Sreenivas Reddy, B: Thermo-diffusion effect on convection heat and mass transfer through a porous medium, (2006), Ph. D thesis, S. K. University, Anantapur, India.

[13] Sreevani, M: Mixed convection heat and mass transfer through a porous medium in channelswith dissipative effects, (2003) Ph. D thesis, S, K. University, Anantpur, India.

[14] Sudha Mathew: Hydro magnetic mixed convective heat and mass transfer through a porous medium in a vertical channel with thermo-diffusion effect. (2009),Ph.D thesis, S,K. University, Anantapur, India.

[15] Sudheer Kumar, Dr. M.P. Singh, Dr. Rajendra Kumar: Radiation effect on natural convection over a vertical cylinder in porous media., (2006), Acta Ciencia Indica, V.XXXII M , No.2.

Figures:

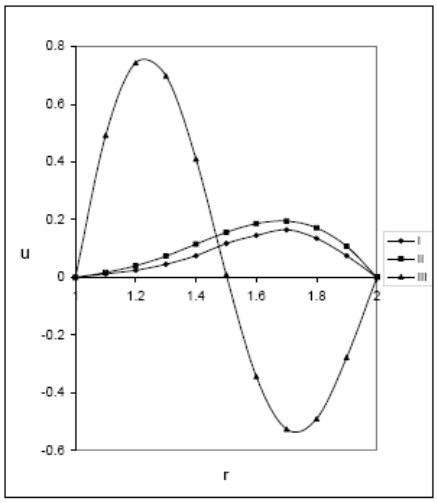

Fig – 1: Variation of u with D^{-1}
N=1,α=2,Sc=1.3, $G=10^3$

	I	II	III
D^{-1}	$5x10^2$	10^3	$2x10^3$

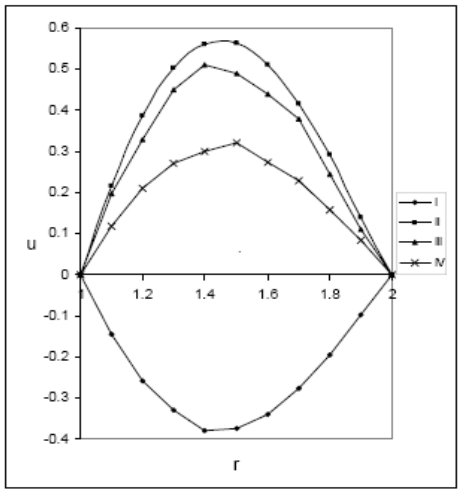

Fig-2: Variation of u with N values
$G=10^3$,$D^{-1}=5x10^2$,Sc=1.3

	I	II	III	IV
N	-0.5	-0.8	1	2

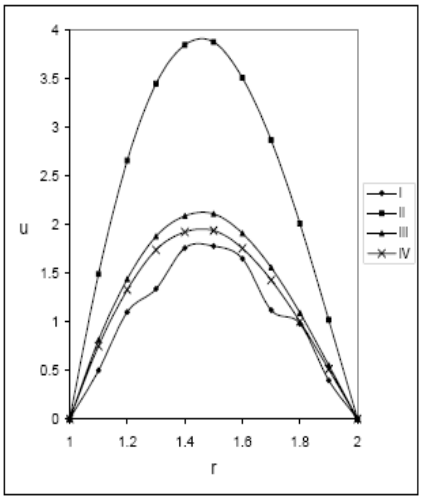

Fig-3: Variation of u with Sc values
$G=10^3$,$D^{-1}=5x10^2$, N=1

	I	II	III	IV
Sc	2.01	0.24	0.6	1.3

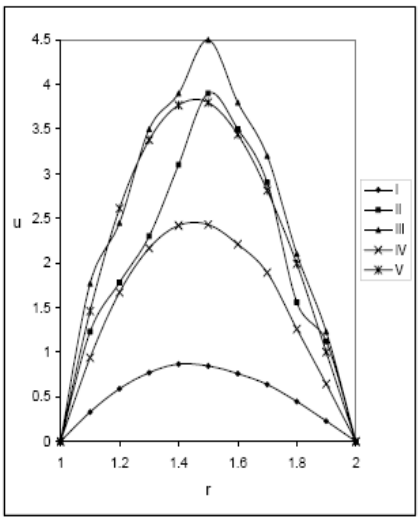

Fig-4: Variation of u with N_1 & N_2 values
$G=10^3$,$D^{-1}=5x10^2$,Sc=1.3

	I	II	III	IV	V
N_1	0.25	0.5	0.75	0.5	0.5
N_2	0.5	0.5	0.5	0.25	0.75

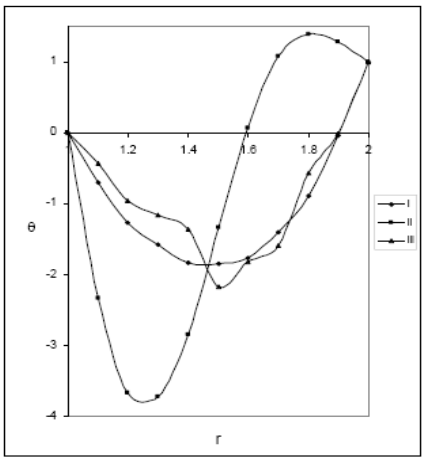

Fig – 5: Variation of θ with D^{-1}
N=1,α=2,Sc=1.3, $G=10^3$

	I	II	III
D^{-1}	$5x10^2$	10^3	$2x10^3$

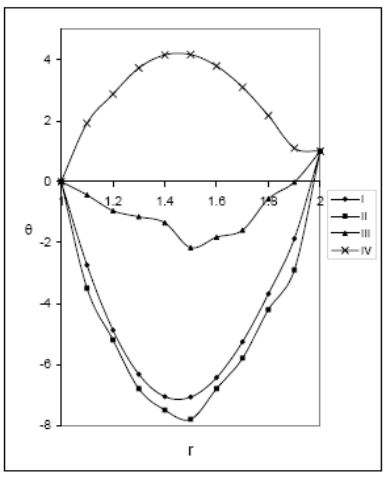

Fig-6: Variation of θ with N values
$G=10^3$,$D^{-1}=5x10^2$,Sc=1.3

	I	II	III	IV
N	-0.5	-0.8	1	2

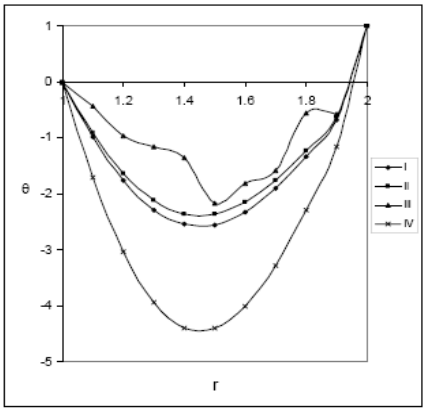

Fig-7: Variation of θ with Sc values
$G=10^3, D^{-1}=5x10^2$, N=1

	I	II	III	IV
Sc	2.01	0.24	0.6	1.3

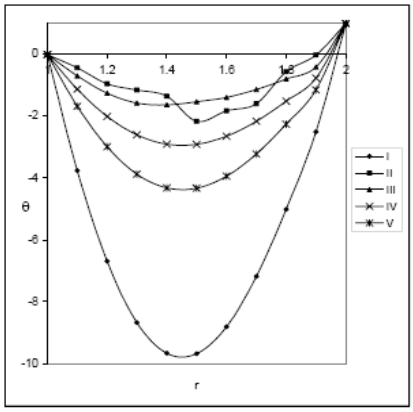

Fig-8: Variation of θ with N_1 & N_2 values
$G=10^3, D^{-1}=5x10^2$, Sc=1.3

	I	II	III	IV	V
N_1	0.25	0.5	0.75	0.5	0.5
N_2	0.5	0.5	0.5	0.25	0.75

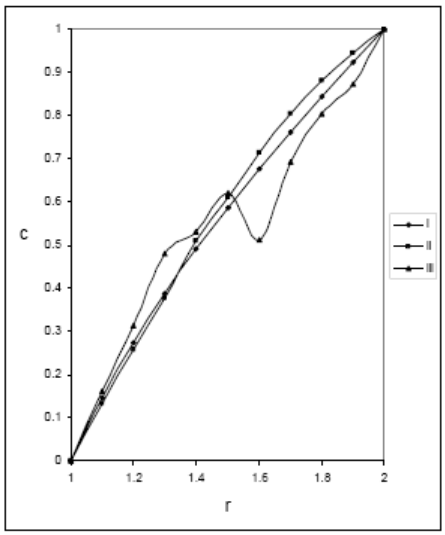

Fig –9: Variation of c with D^{-1}
N=1, α=2, Sc=1.3, $G=10^3$

	I	II	III
D^{-1}	$5x10^2$	10^3	$2x10^3$

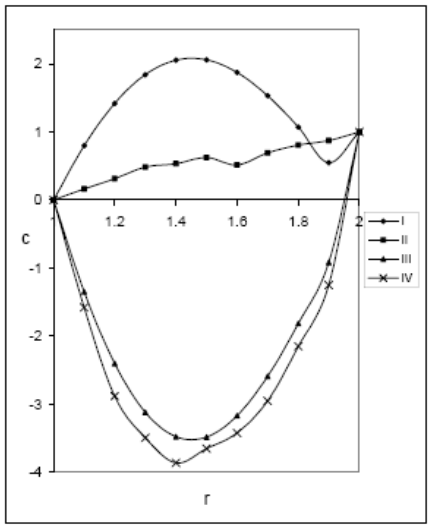

Fig-10: Variation of c with N values
$G=10^3, D^{-1}=5x10^2$, Sc=1.3

	I	II	III	IV
N	-0.5	-0.8	1	2

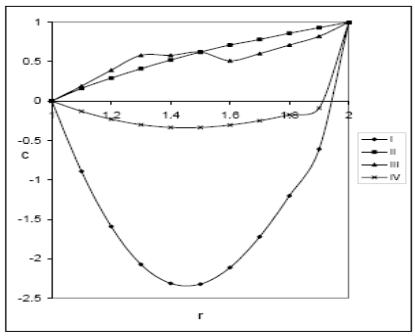

Fig-11: Variation of θ with Sc values
$G=10^3, D^{-1}=5x10^2$, N=1

	I	II	III	IV
Sc	2.01	0.24	0.6	1.3

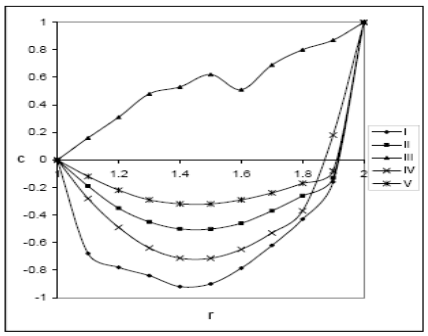

Fig-12: Variation of θ with N_1 & N_2 values
$G=10^3, D^{-1}=5x10^2$, Sc=1.3

	I	II	III	IV	V
N_1	0.25	0.5	0.75	0.5	0.5
N_2	0.5	0.5	0.5	0.25	0.75

Tables:

Table.1
Shear Stress(τ) at r=1
P=0.71, N_T=0.5,N_C=0.5

D^{-1}	I	II	III	IV	V	VI	VII	VIII	IX	X
10^2	-0.0751009	-0.184662	0.0733353	0.290926	-0.0750264	-0.0752079	-0.0751715	-0.0119477	-0.117574	-0.130572
$3X10^2$	-0.0784576	-0.191546	0.0773526	0.312053	-0.0783786	-0.078576	-0.0785358	-0.0114721	-0.123525	-0.137329
$5X10^2$	-0.0821667	-0.199026	0.0818961	0.336908	-0.0820788	-0.0822983	-0.0822535	-0.0109081	-0.13013	-0.144835
G	10^2	$3X10^2$	$-1X10^2$	$-3X10^2$	10^2	10^2	10^2	10^2	10^2	10^2
Sc	1.3	1.3	1.3	1.3	2.01	0.24	0.6	1.3	1.3	1.3
N	1	1	1	1	1	1	1	2	-0.5	-0.8

Table.2
Shear Stress (τ) at r=1
G=10^2,S_C=1.3,N=0.5

D^{-1}	I	II	III	IV	V
10^2	-0.0780199	-0.0751009	-0.0724137	-0.075166	-0.07503
$3X10^2$	-0.0816818	-0.0784576	-0.075503	-0.0785302	-0.078385
$5X10^2$	-0.0857485	-0.0821667	-0.0789009	-0.082247	-0.082086
N_1	0.25	0.5	0.75	0.5	0.5
N_2	0.5	0.5	0.5	0.25	0.75

Table.3
Shear Stress(τ) at r=2
P=0.71, N_T=0.5,N_C=0.5

D^{-1}	I	II	III	IV	V	VI	VII	VIII	IX	X
10^2	0.0116307	0.011908	-0.00778866	-0.0649968	0.0115878	0.0116948	0.011673	-0.0663988	0.0638844	0.0797217
$3X10^2$	0.0133867	0.0148555	-0.00991133	-0.0769352	0.0133392	0.0134578	0.0134336	-0.0674132	0.0675124	0.0839285
$5X10^2$	0.0153543	0.0185525	-0.0123525	-0.091167	0.0153013	0.0154336	0.0154066	-0.0685005	0.0715468	0.0886019
G	10^2	$3X10^2$	$-1X10^2$	$-3X10^2$	10^2	10^2	10^2	10^2	10^2	10^2
Sc	1.3	1.3	1.3	1.3	2.01	0.24	0.6	1.3	1.3	1.3
N	1	1	1	1	1	1	1	2	-0.5	-0.8

Table.4
Shear Stress(τ) at r=2
G=10^2,S_C=1.3,N=0.5

D^{-1}	I	II	III	IV	V
10^2	0.0131563	0.0116307	0.0102436	0.01167	0.0115914
$3X10^2$	0.0150955	0.0133867	0.0118397	0.0134303	0.0133432
$5X10^2$	0.0172789	0.0153543	0.0136204	0.0154029	0.0153058
N_1	0.25	0.5	0.75	0.5	0.5
N_2	0.5	0.5	0.5	0.25	0.75

Table.5
Nusselt Number(Nu) at r=1
P=0.71, N_T=0.5,N_C=0.5

D^{-1}	I	II	III	IV	V	VI	VII	VIII	IX	X
10^2	-4.15092	-3.76746	-4.67044	-5.43201	-4.15117	-4.15054	-4.15067	-4.37195	-4.00226	-3.9576
$3X10^2$	-4.13917	-3.74336	-4.6845	-5.50595	-4.13944	-4.13875	-4.13889	-4.37362	-3.98143	-3.93312
$5X10^2$	-4.12619	-3.71719	-4.70041	-5.59298	-4.12649	-4.12573	-4.12588	-4.37559	-3.95831	-3.90885
G	10^2	$3X10^2$	$-1X10^2$	$-3X10^2$	10^2	10^2	10^2	10^2	10^2	10^2
Sc	1.3	1.3	1.3	1.3	2.01	0.24	0.6	1.3	1.3	1.3
N	1	1	1	1	1	1	1	2	-0.5	-0.8

Table.6
Nusselt Number(Nu) at r=1
$G=10^2$,S_C=1.3,N=0.5

D^{-1}	I	II	III	IV	V
10^2	-4.15092	-4.27723	-4.0336	-4.15069	-4.15115
$3X10^2$	-4.13917	-4.27083	-4.01738	-4.13891	-4.13942
$5X10^2$	-4.12619	-4.26371	-3.99954	-4.1259	-4.12647
N1	0.5	0.25	0.75	0.5	0.5
N2	0.5	0.5	0.5	0.25	0.75

Table.7
Nusselt Number(Nu) at r=2
P=0.71, N_T=0.5,N_C=0.5

D^{-1}	I	II	III	IV	V	VI	VII	VIII	IX	X
10^2	4.2128	4.21323	4.28077	4.481	4.21295	4.21258	4.21265	4.48591	4.02991	3.97448
$3X10^2$	4.20666	4.20152	4.2882	4.52278	4.20682	4.20641	4.20649	4.48946	4.01722	3.95976
$5X10^2$	4.19977	4.18858	4.29674	4.57259	4.19995	4.19949	4.19959	4.49326	4.0031	3.9434
G	10^2	$3X10^2$	$-1X10^2$	$-3X10^2$	10^2	10^2	10^2	10^2	10^2	10^2
Sc	1.3	1.3	1.3	1.3	2.01	0.24	0.6	1.3	1.3	1.3
N	1	1	1	1	1	1	1	2	-0.5	-0.8

Table.8
Nusselt Number(Nu) at r=2
$G=10^2$,S_C=1.3,N=0.5

D^{-1}	I	II	III	IV	V
10^2	4.23049	4.2128	4.19973	4.21266	4.21294
$3X10^2$	4.22709	4.20666	4.19135	4.2065	4.20681
$5X10^2$	4.22327	4.19977	4.182	4.1996	4.19994
N_1	0.25	0.5	0.75	0.5	0.5
N_2	0.5	0.5	0.5	0.25	0.75

Source of support: Nil, Conflict of interest: None Declared

